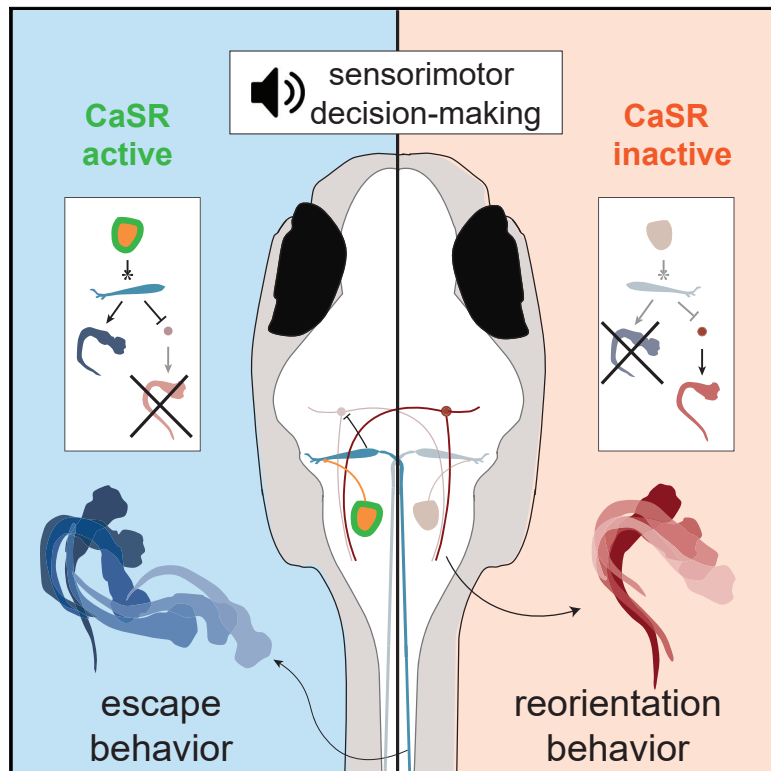**Article**

The *calcium-sensing receptor (CaSR)* regulates zebrafish sensorimotor decision making via a genetically defined cluster of hindbrain neurons

Graphical abstract

Authors

Hannah Shoenhard, Roshan A. Jain, Michael Granato

Correspondence

granatom@pennmedicine.upenn.edu

In brief

Work by Shoenhard et al. illustrates a rare example of a G-protein-coupled receptor that acutely biases vertebrate sensorimotor decision making via a genetically defined neuronal cluster in the hindbrain.

Highlights

- *CaSR* mutant zebrafish larvae exhibit deficits in sensorimotor decision making

- CaSR functions acutely to regulate decision making

- CaSR functions in a small, molecularly defined hindbrain cluster

- CaSR expression is both required and sufficient to bias decision making

CellPress

Article

The *calcium-sensing receptor (CaSR)* regulates zebrafish sensorimotor decision making via a genetically defined cluster of hindbrain neurons

Hannah Shoenhard,[1] Roshan A. Jain,[2] and Michael Granato[1,3,*]
[1]Department of Cell and Developmental Biology, Perelman School of Medicine, University of Pennsylvania, Philadelphia, PA 19104, USA
[2]Department of Biology, Haverford College, Haverford, PA 19041, USA
[3]Lead contact
*Correspondence: granatom@pennmedicine.upenn.edu
https://doi.org/10.1016/j.celrep.2022.111790

SUMMARY

Decision making is a fundamental nervous system function that ranges widely in complexity and speed of execution. We previously established larval zebrafish as a model for sensorimotor decision making and identified the G-protein-coupled *calcium-sensing receptor* (*CaSR*) to be critical for this process. Here, we report that *CaSR* functions in neurons to dynamically regulate the bias between two behavioral outcomes: escapes and reorientations. By employing a computational guided transgenic strategy, we identify a genetically defined neuronal cluster in the hindbrain as a key candidate site for CaSR function. Finally, we demonstrate that transgenic CaSR expression targeting this cluster consisting of a few hundred neurons shifts behavioral bias in wild-type animals and restores decision making deficits in *CaSR* mutants. Combined, our data provide a rare example of a G-protein-coupled receptor that biases vertebrate sensorimotor decision making via a defined neuronal cluster.

INTRODUCTION

A critical function of the nervous system is to continuously make decisions, ranging from goal-oriented or conceptual decision making to more instant and simpler forms of decision making. One relatively simple form of decision making, known as sensorimotor decision making, occurs when animals sense an abrupt sensory stimulus and instantly select between several motor responses. Over the past decades, numerous assays to measure and quantify decision making in genetically tractable invertebrate and vertebrate models have been established.[1–12] This has led to the identification of genetic pathways that regulate decision making,[4,7,13–16] yet a long-standing quest in the field has been to identify the neural circuitry through which these genetic pathways regulate decision making in the vertebrate brain. We previously established a high-throughput behavioral assay to measure sensorimotor decision making in larval zebrafish. Exposure to a sudden acoustic stimulus triggers either a rapid escape behavior (the short-latency C-start, or SLC) or a slower reorientation maneuver (the long-latency C-start, or LLC).[17] Response selection depends greatly on stimulus quality, with high-intensity stimuli (>35dB) resulting in an escape response and low-intensity stimuli (<25dB) predominantly resulting in a reorientation behavior. Importantly, response selection is modulated not only by stimulus quality but also by stimulus history, as well as by neuromodulatory systems, all hallmarks of more complex decision making.[18] From a forward genetic screen coupled with whole-genome sequencing we identified the G-protein-coupled *cal-cium-sensing receptor* (*CaSR*) to be critical for sensorimotor decision making.[18] *CaSR* loss-of-function mutants perform predominantly reorientation behaviors in response to acoustic stimuli that in wild-type siblings evoke the escape response. Conversely, responses to low-intensity stimuli that evoke the reorientation behavior from wild-type larvae are shifted toward the escape response in larvae treated with a pharmacological CaSR agonist.[18] Taken together, these data strongly suggest that CaSR functions as a bidirectional regulator of decision making: decreased CaSR signaling drives bias toward reorientations, while increased CaSR signaling drives bias toward escapes.

CaSR is a G-protein-coupled receptor that spans the plasma membrane and detects extracellular calcium levels.[19] CaSR is highly conserved in vertebrates[20] and has been extensively studied for its role in maintaining serum calcium homeostasis.[21–23] CaSR also contributes to nervous system development[24–27] and plays an acute role in nervous system function including in synaptic transmission.[28,29] In a wide array of cell types including neurons and astrocytes,[30] CaSR facilitates acute adaptation to changing extracellular calcium concentrations. For example, in mouse neocortical and hippocampal axon terminals, CaSR signaling partially compensates for low extracellular calcium by potentiating non-selective cation currents,[31,32] possibly allowing evoked vesicle release to succeed under a wider range of extracellular concentrations.[33] Finally, in mice, CaSR activation also facilitates oligodendrocyte differentiation.[24,34] In contrast, the cell types and neural circuitry through which CaSR regulates sensorimotor decision making have not been identified.

Here, we determine when and where in the zebrafish CaSR regulates sensorimotor decision making. We provide compelling genetic evidence that CaSR is dispensable during circuit development and instead regulates sensorimotor decision making acutely, consistent with previous pharmacological data.[18] We show that for sensorimotor decision making, CaSR function is dispensable in sensory hair cells and glial cell types and instead acts in neurons. Moreover, we find that CaSR function is dispensable in multiple neuronal populations that regulate and execute the escape and reorientation behaviors. Instead, using an unbiased computationally guided transgenic strategy, we identify the dorsal cluster rhombomere 6 (DCR6) region, a hindbrain cluster of several hundred neurons, as a likely candidate site for CaSR function. We show that transgenic expression of CaSR in a defined population of hindbrain neurons shifts behavioral bias in wild-type animals and restores decision-making deficits in *CaSR* mutants, providing compelling evidence that this population is a key site for CaSR function. Finally, using a sparse neuronal labeling strategy, we identify axonal projections that connect this cluster to escape circuit neurons, providing a potential circuit mechanism via which this population might influence initiation of the escape behavior. Combined, our data provide a rare example of a vertebrate-specific G-protein-coupled receptor that regulates sensorimotor decision making via a genetically defined hindbrain neuronal population.

RESULTS

The G-protein-coupled receptor CaSR acts acutely to regulate decision making

CaSR is widely expressed throughout neural development and is also detectable later during the time period when larvae display sensorimotor decision making.[22,23] We therefore determined whether CaSR acts during neural circuit assembly or more acutely during the process of sensorimotor decision making. For this, we generated the transgenic line *Tg(hsp70:CaSR-EGFP, myl7:GFP)* in which heat shock treatment induces ubiquitous CaSR-EGFP expression. In zebrafish, the assembly of the neural circuits that mediate escape as well as reorientation behaviors is largely complete by 4 days post fertilization (dpf).[35] Moreover, sensorimotor decision making that dynamically regulates the bias between escape and reorientation behaviors is robustly observed by 4 dpf. We therefore induced CaSR-EGFP expression in otherwise *CaSR* mutant larvae at three timepoints: prior to 4 dpf, at 4 dpf, and at 5 dpf (Figure 1A). Inducing transgenic CaSR-EGFP expression in *CaSR* mutant larvae prior to 4 dpf failed to restore subsequent sensorimotor decision making (Figure 1C). In contrast, inducing CaSR-GFP expression at 4 dpf resulted in complete behavioral rescue at 5 dpf, so mutant larvae exhibited sensorimotor decision making indistinguishable from sibling controls (Figure 1D). Moreover, inducing CaSR-EGFP expression at 5 dpf in *CaSR* mutants already exhibiting defects in decision making restored this process to wild-type levels at 6 dpf (Figure 1E). Combined, these results provide compelling genetic evidence that CaSR function is dispensable for circuit development and instead regulates sensorimotor decision making dynamically via an acute mechanism.

CaSR acts independent of neuronal circuits mediating escape and reorientation behaviors

In vertebrates, CaSR is expressed in neurons,[33] hair cells,[36] and various glial cell types including astrocytes[30] and oligodendrocytes.[34] To determine the cell type(s) in which CaSR functions to regulate sensorimotor decision making, we utilized a transgenic rescue approach. Specifically, we took advantage of the ability of the CaSR-EGFP transgene to restore sensorimotor decision making when expressed ubiquitously (Figure 1), and used the Gal4/UAS system[37] to restrict CaSR-EGFP expression to specific cell types. We first tested whether CaSR-EGFP expression in glial cell types or neurons is sufficient to restore sensorimotor decision making in otherwise *CaSR* mutant animals. We confirmed CaSR expression via GFP expression from the *CaSR-EGFP* transgene and compared sensorimotor decision making in *CaSR* mutants in the absence or presence of cell type-specific CaSR-EGFP expression. Transgenic CaSR-EGFP expression in astrocytes or oligodendrocyte-lineage cells failed to restore decision-making bias (Figure 2). Similarly, transgenic CaSR-EGFP expression in hair cells critical for auditory function underlying both escape and reorientation behaviors also failed to restore decision making in *CaSR* mutants (Figure 2). In contrast, transgenic CaSR-EGFP expression in neurons using a pan-neuronal promotor (*αtubulin:Gal4>UAS:CaSR-EGFP*) significantly shifted decision-making bias in *CaSR* mutants toward escapes (Figure 2), providing compelling evidence that CaSR regulates decision making through a neuronal pathway.

Several neuronal populations critical for escape behaviors[17,38–42] as well as a key population mediating reorientation behaviors[43] have previously been identified (Figure 3A). Given that CaSR regulates the bias between escape (SLC) and reorientation (LLC) behaviors, we first tested whether neuronal populations known to mediate SLC and LLC behaviors mediate CaSR-dependent decision making. Using the same Gal4>UAS:CaSR-EGFP transgenic approach, we tested if CaSR-EGFP expression in neurons involved in SLC or LLC circuits in otherwise *CaSR* mutant animals restores decision making. Transgenic expression of CaSR-EGFP in SLC circuit neurons including the Mauthner neuron (*Et(GFFDMC130a)*),[44] glycinergic inhibitory neurons (*Tg(GlyT2:Gal4,myl7:GFP)*),[45,46] spiral fiber neurons (*Tg(-6.7FRhcrtR:gal4VP16)*),[41] as well as LLC-mediating prepontine neurons (*Et(y293:Gal4)*)[43] failed to restore decision making (Figure 3B). Finally, we tested whether serotonergic neurons in the dorsal raphe previously shown to represent internal states in zebrafish foraging behaviors[47] and to regulate certain forms of decision making in mice[48] function in CaSR-dependent sensorimotor decision making. Expression of *fev:Gal4>UAS:CaSR-EGFP* in serotonergic neurons in the dorsal raphe[49] failed to restore CaSR-dependent decision making (Figure 3B). We cannot exclude the possibility that the Gal4 driver lines we used express at levels too low to restore CaSR function and/or might fail to express in all neurons of the population we targeted. Nonetheless, combined, our data strongly suggest that CaSR regulates decision making independent of known neuronal populations critical for SLC and LLC behaviors, and instead it might act in other neuronal populations.
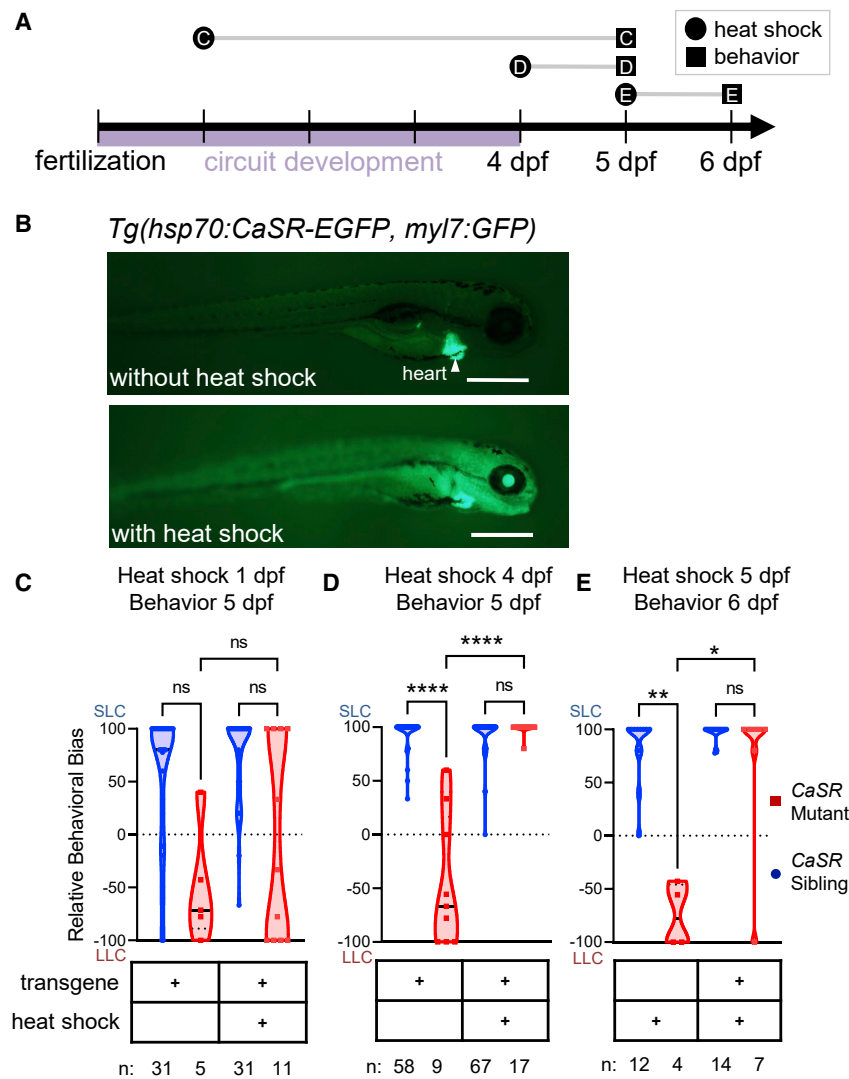
Figure 1. CaSR expression after development of behaviorally relevant circuits is sufficient to restore decision making in *CaSR* mutants

(A) Timeline of zebrafish escape and reorientation circuit development. Both behaviors have emerged by 4 dpf. Letters correspond to panels in this figure. Circles indicate time of heat shock; squares indicate time of behavioral testing.

(B) Fluorescent image of *Tg(hsp70:CaSR-EGFP, myl7:GFP)* larva without (top) and with (bottom) heat shock. Arrow indicates heart label used for embryo pre-sorting. Scale bar represents 500 um.

(C) Average relative startle bias of 5 days post-fertilization (dpf) sibling and mutant *Tg(hsp70:CaSR-EGFP,myl7:GFP)* larvae subject to no heat shock or to heat shock at 1 dpf. Blue circles indicate *CaSR* WT and heterozygous siblings; red squares indicate *CaSR* homozygous mutants. n.s. incidates $p > 0.05$.

(D) Average relative startle bias of 5 days post-fertilization (dpf) sibling and mutant *Tg(hsp70:CaSR-EGFP,myl7:GFP)* larvae subject to no heat shock or to heat shock at 4 dpf. Results are from three experiments. **** incidates $p < 0.0001$. n.s. incidates $p > 0.05$.

(E) Average relative startle bias of 6 dpf sibling and mutant *Tg(hsp70:CaSR-EGFP,myl7:GFP)* larvae subject to no heat shock or to heat shock at 5 dpf. No transgene control siblings vs. mutants $p = 0.007$. No transgene control vs. transgenic mutants, $p = 0.0145$. n.s. incidates $p > 0.05$. In (C), (D), and (E), solid lines indicate median; dashed lines indicate quartiles. All p values in (C), (D), and (E) are from Kruskal-Wallis test with Dunn's multiple comparisons post hoc test.

A neuronal cluster in the dorsal rhombomere 6 of the hindbrain is associated with CaSR-dependent decision making

The broad expression of CaSR throughout the brain and the absence of compelling candidate neuronal populations dissuaded us from testing additional neuronal populations based on gene expression or literature predictions. Instead, we developed a more unbiased strategy that requires no prior knowledge of the neuronal population in which CaSR is expressed and acts. For this we took advantage of several observations. First, we had previously shown that acute treatment of wild-type larvae with CaSR-specific agonists produces the opposite of the *CaSR* mutant phenotype, biasing behavioral responses at low stimulus intensities to escapes to a degree that is typically evoked only by high-intensity stimuli.[18] Conversely, reduced CaSR signaling, either in *CaSR* loss-of-function mutants or via treatment of wild-type larvae with CaSR-specific antagonists, biases behavioral responses at high stimulus intensities to reorientations that typically predominate at low-intensity stimuli.[18] Together, these observa-

tions support the idea that CaSR activity is required and sufficient to shift the bias between escape and reorientation behaviors. Second, we find that transgenic CaSR expression in neurons using *αtubulin:Gal4>UAS:CaSR-EGFP* restored decision making in *CaSR* mutants (Figures 2 and 4B). Third, pan-neuronal overexpression of CaSR-EGFP in wild-type and *CaSR* heterozygous larvae significantly shifts decision-making bias toward performing escapes following low-intensity stimuli (Figure 4C), consistent with pharmacological data suggesting CaSR functions as a bidirectional regulator of sensorimotor decision making.[18] Finally, in zebrafish the Gal4/UAS system is known to frequently result in variegated expression patterns through epigenetic silencing of the UAS, producing incomplete expression throughout the target tissue that varies between individual animals.[50,51] In fact, we observed variable expression levels and patterns in individual *αtubulin:Gal4>UAS:CaSR-EGFP* larvae and found that the ability of transgenic CaSR-EGFP expression to bias decision making in both mutants and siblings was highly variable and correlated with the expression levels of *CaSR-EGFP* (Figures 4B–4D). Combined, these observations prompted us to harness the variability of the CaSR-EGFP expression pattern to identify candidate cell populations in which *CaSR* levels influence decision-making bias.
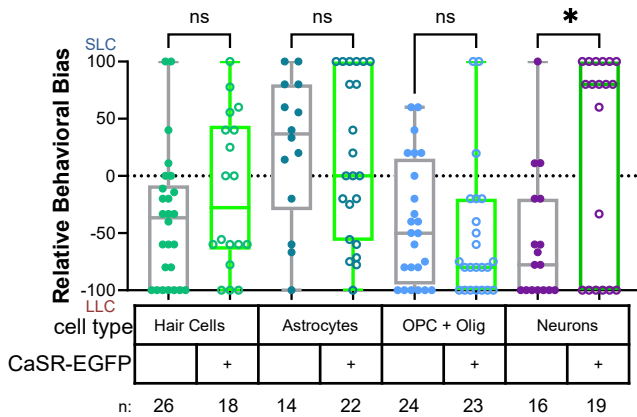
Figure 2. Transgenic CaSR expression in neurons, but not other cell types, restores decision making in *CaSR* mutants

Relative behavioral bias of *CaSR* mutant larvae either not expressing (filled circle, gray box and whiskers) or expressing (empty circle, green box and whiskers) UAS:CaSR-EGFP in the indicated cell type. Cyan, hair cells; dark blue, astrocytes; sky blue, OPCS and oligodendrocytes; purple, neurons. CaSR-EGFP negative control larvae vs. neuronal CaSR-EGFP larvae p = 0.0168. n.s. indicates p > 0.05. Lines indicate median; box extends from 25th to 75th percentile. p values are from Kruskal-Wallis test with Dunn's multiple comparisons post hoc test.

For this we developed a computational approach, which we termed multivariate analysis of variegated expression in neurons (MAVEN), to assess how CaSR-EGFP expression levels within anatomically and molecularly defined brain regions of individual larvae correlate with their decision-making bias (Figure 5A). Specifically, we classified the relative behavioral bias of 140 individual *αtubulin:Gal4>UAS:CaSR-EGFP* larvae as either "SLC-shifted" or "not SLC-shifted" in response to low-intensity acoustic stimuli. We then imaged the CaSR-EGFP expression pattern in the entire brain of these larvae using a confocal microscope and registered each brain to the 3D zebrafish brain reference atlas (3D ZBrain;[52] see STAR Methods). Next, to uncover correlations between CaSR-EGFP signal intensity in specific brain regions in individual larvae and their shift from reorientations (LLC) to escapes (SLC), we used LASSO regression, a form of multivariate analysis.[53] From 251 distinct brain regions, this approach identified a single brain region, the "Rhombencephalon QRFP Cluster – Sparse," henceforth referred to as dorsal cluster rhombomere 6 or DCR6, to be strongly correlated with a CaSR-dependent shift from reorientation (LLC) to escape (SLC) responses. The DCR6 region is located in rhombomere 6 dorsal to the Mauthner neuron, and it is estimated to consist of a few hundred neurons with about half of these neurons expressing VGlut2 (Figure 5B) (https://zebrafishatlas.zib.de/ [54]). Finally, we performed two-way ANOVA to assess if "SLC-shifted" larvae (n = 36 wild-type, 40 heterozygote, and 5 mutant larvae) had higher levels of CaSR-EGFP in the DCR6 region compared with "not SLC-shifted" larvae (n = 14 wild-type, 40 heterozygote, and 6 mutant larvae). This revealed a highly significant association between the CaSR-EGFP signal in the DCR6 and SLC bias (p < 0.0001), further suggesting the DCR6 region is functionally important for CaSR-dependent decision making (Figure 5C).
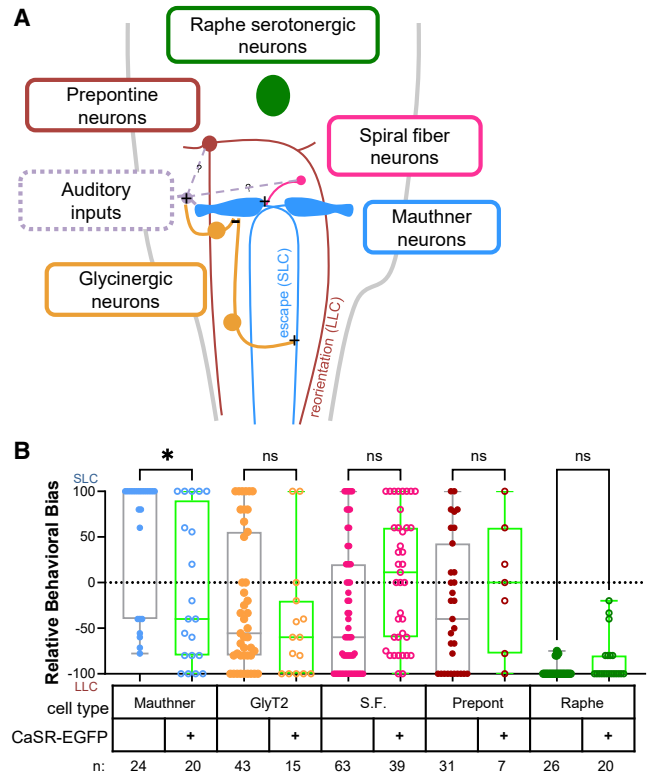

Figure 3. CaSR re-expression in known escape (SLC) and reorientation (LLC) circuit components fails to rescue decision making in *CaSR* mutants

(A) Diagram of circuit relationships of SLC and LLC circuit components. Blue, Mauthner; orange, glycincergic neurons including feedforward and feedback inhibitory neurons; pink, spiral fiber feedforward excitatory neurons; brick red, prepontine LLC-mediating neurons; green, serotonergic neurons of the Raphe.

(B) Relative behavioral bias of *CaSR* mutant larvae either not expressing (filled circle, gray box and whiskers) or expressing (empty circle, green box and whiskers) UAS:CaSR-EGFP in the indicated cell type. Colors as in (A). CaSR-EGFP negative control larvae versus Mauthner CaSR-EGFP larvae p = 0.0294; note that these larvae were shifted toward reorientations, the opposite direction expected from behavioral rescue. n.s. indicates p > 0.05. Lines indicate median, box extends from 25th to 75th percentile. p values are from Kruskal-Wallis test with Dunn's multiple comparisons post hoc test.

CaSR expression in the y234/DRC6 neurons is sufficient and required for sensorimotor decision making

Our finding that CaSR expression levels in the DCR6 cluster correlate with a shift toward the escape behavior identified this cluster as a strong candidate site for CaSR-dependent sensorimotor decision making. To further validate this correlative result, we selected from the ZBrain 2.0 atlas (https://zebrafishatlas.zib.de/) a Gal4 line *Et(y234:Gal4)*[55] that drives expression in and immediately surrounding the DCR6 cluster (Figure 6A). We then performed both gain- and loss-of-function experiments to determine whether CaSR-EGFP expression in *y234*-labeled neurons of the DCR6 cluster (y234/DCR6 neurons) is sufficient and required for sensorimotor decision making. Expression of CaSR in y234/DRC6 neurons was sufficient to shift decision-making bias from reorientation to escape responses in *CaSR* sibling
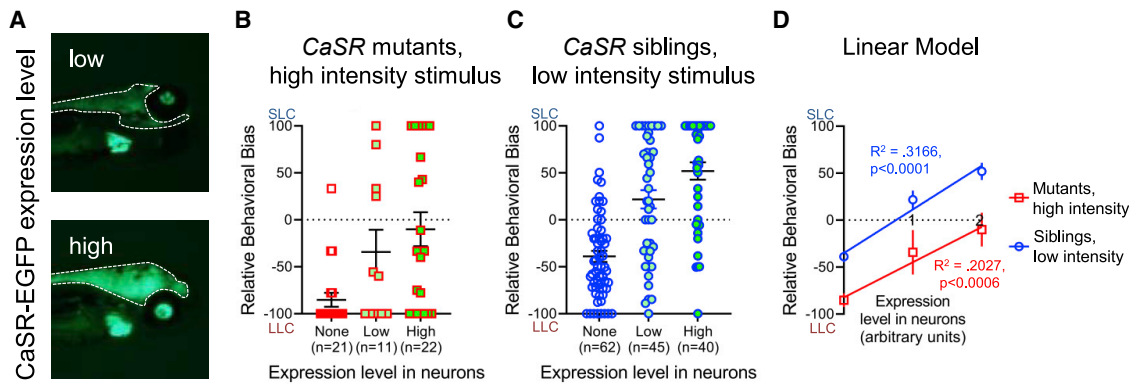
Figure 4. Neuronal CaSR expression shifts decision making in *CaSR* mutants and siblings in a dose-dependent manner

(A) Brains and rostral spinal cords of larvae expressing CaSR-EGFP under control of the αTub:Gal4 driver, outlined with white dashed line. Since the αTubulin:Gal4 line also includes a myl7:GFP marker, green hearts are also visible. Top, representative example of a fish from the "low expression" category. Bottom, representative example of a fish from the "high expression" category.

(B) Relative behavioral bias in response to strong acoustic stimuli of *CaSR* mutants not expressing any CaSR-EGFP (no fill), manually sorted into the "low expression" category (light green fill), or manually sorted into the "high expression" category (bright green fill). Lines represent means +/− SEM.

(C) Relative behavioral bias in response to weak acoustic stimuli of *CaSR* siblings not expressing any CaSR-EGFP (no fill), manually sorted into the "low expression" category (light green fill), or manually sorted into the "high expression" category (bright green fill). Lines represent means +/− SEM.

(D) Univariate linear models of effects of CaSR-EGFP expression levels in neurons on relative behavioral bias. For the X axis, arbitrary units were used, with 0 corresponding to no CaSR-EGFP expression, 1 to low CaSR-EGFP expression, and 2 to high CaSR-EGFP expression. Red squares, *CaSR* mutants (from B). Blue circles, *CaSR* siblings (from C). Mutant linear model slope significantly different from 0, p = 0.0006; R^2 = 0.2027. Sibling linear model slope significantly different from 0, p < 0.0001; R^2 = 0.3166.

larvae exposed to low-intensity stimuli (Figure 6B). Importantly, the y234:Gal4 line also drives expression in the trigeminal and vagal ganglia (Figure 6A). To assess the potential contribution of CaSR expression in the trigeminal and vagal ganglia in our decision-making paradigm, we used the y293:Gal4 line, which drives expression in the prepontine reorientation-mediating neurons (Figure 3), the trigeminal ganglia, and the vagal ganglia, but not the DCR6 cluster (Figure 6C). Driving CaSR-EGFP using the y293:Gal4 line failed to shift behavioral bias (Figure 6D), consistent with the idea that the y234/DCR6 cluster, not the trigeminal and/or vagal ganglia, is a key site for CaSR-dependent decision making.

We next asked whether CaSR expression in y234/DCR6 neurons was sufficient to restore sensorimotor decision making in otherwise *CaSR* mutant animals. As expected, when exposed to high-intensity stimuli, *CaSR* siblings in the presence or absence of *y234:Gal4>UAS CaSR-EGFP* predominantly perform escape (SLC) behaviors, while *CaSR* mutants lacking *y234:Gal4>UAS CaSR-EGFP* predominantly perform reorientation (LLC) behaviors (Figure 6E). In contrast, *y234:Gal4>UAS:CaSR-EGFP* expression in *CaSR* mutants significantly shifts decision-making bias toward escapes (Figure 6E), reversing the *CaSR* mutant phenotype. Importantly, using the y293:Gal4 line to drive CaSR-EGFP in the prepontine neurons, trigeminal ganglia, and vagal ganglia but not in the y234/DCR6 of *CaSR* mutants failed to restore CaSR-dependent decision making (Figure 3B). Combined, these results demonstrate that transgenic CaSR expression in y234/DCR6 neurons is both sufficient to bias decision making in *CaSR* sibling larvae and to restore this process in *CaSR* mutants, strongly suggesting that CaSR function in y234/DCR6 neurons is required for proper decision-making bias. Moreover, our results reveal a role for y234/DCR6 neurons in regulating decision making between

escape and reorientation behaviors. Finally, our data provide compelling evidence that CaSR is a key regulator of y234/DCR6-mediated sensorimotor decision making.

Having identified y234/DCR6 neurons to be critical for CaSR-dependent bias between escape and reorientation behaviors, we asked whether y234/DCR6 neurons connect to prepontine neurons of the reorientation circuit (Figure 3A) or neurons of the escape circuit. For this we used the *y234:Gal4*; *UAS: gap43-citrine*[56] lines that sparsely labeled y234/DCR6 neurons and their axonal projections. While we failed to detect axon projections extending toward the prepontine brain, we identified a population of y234/DCR6 neurons whose axons projected toward the Mauthner neuron. Simultaneously visualizing y234/DCR6 neurons in conjunction with Mauthner neurons using the *Tg(hspGFF62a:Gal4)*[57] line revealed that in 6/13 larvae analyzed, these y234/DCR6 neurons project to the lateral dendrite of the Mauthner neuron, a critical site for initiating acoustically evoked escape behaviors[58,59] (Figures 6F and 6G). Although the circuit functionality of these y234/DCR6 projections has yet to be established, our data point to the intriguing possibility that these axonal projections connect y234/DCR6 neurons to the Mauthner neuron escape circuit, providing a possible mechanism by which *y234:Gal4*-driven CaSR expression in the y234/DCR6 influences escape bias. Independent of the precise circuit mechanism, our data provide compelling evidence that CaSR is a key regulator of y234/DCR6-mediated sensorimotor decision making.

DISCUSSION

Sensorimotor decision making is an evolutionarily conserved process that requires the nervous system to integrate stimulus qualities, prior experiences, ongoing behaviors, and internal
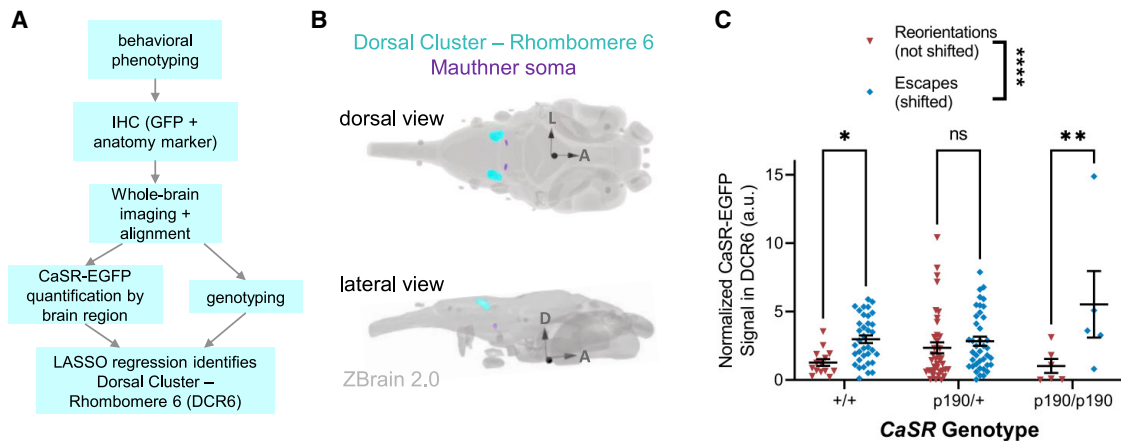
Figure 5. Multivariate analysis of variegated expression in neurons (MAVEN) identifies a hindbrain region where CaSR overexpression correlates with decision-making phenotype

(A) Experimental workflow for MAVEN experiment.

(B) Location of the dorsal cluster rhombomere 6 (cyan), relative to the Mauthner soma (purple), in rhombomere 4. Image generated using ZBrain 2.0's 3D Viewer tool (https://zebrafishatlas.zib.de/).

(C) Normalized fluorescence intensity signal in the dorsal cluster rhombomere 6 in brightly expressing *αTubulin:Gal4; UAS:CaSR-EGFP; CaSR*[p190/+] larvae of various *CaSR* genotypes that were SLC-shifted in response to a weak, primarily LLC-evoking stimulus. Two-way ANOVA column factor (phenotype) p < 0.0001. Non-shifted vs. escape-shifted wild-type larvae p = 0.0462. Non-shifted vs. escape-shifted mutant larvae p = 0.0027. n.s. indicates p > 0.05. Multiple comparisons were controlled using Sidak's multiple comparison's test. Lines represent mean +/− SEM.

states such as hunger or anxiety.[2,6,7,60–65] While the behavioral parameters and circuit correlates of many forms of sensorimotor decision making have been well characterized in invertebrate and vertebrate systems,[3,66–68] the neuronal populations in which individual molecular-genetic pathways regulate decision-making processes in the vertebrate brain are not well defined. Using zebrafish, we previously demonstrated that the calcium-sensing G-protein-coupled receptor CaSR is required to regulate bias between two acoustically evoked and mutually exclusive behavioral outcomes: a rapid escape behavior (the SLC) and a slower reorientation behavior (the LLC).[18] Here we provide compelling genetic evidence that CaSR biases this decision process acutely via a small, genetically defined cluster of hindbrain neurons. Our results represent a rare example of a G-protein-coupled receptor that biases vertebrate sensorimotor decision making via a genetically defined neuronal cluster.

CaSR biases sensorimotor decision making via a genetically defined hindbrain cluster

Multiple lines of evidence support the conclusion that CaSR acts in y234/DCR6 neurons to acutely and bidirectionally regulate decision-making bias. First, transgenic CaSR expression in astrocytes, oligodendrocytes, or hair cells failed to restore decision making in otherwise mutant animals, while CaSR expression in neurons did, demonstrating a neuronal role for CaSR in decision making (Figure 2). Moreover, transgenic CaSR expression in neurons of *CaSR* sibling larvae dose dependently biased decision making in response to low-intensity stimuli toward escape responses (Figure 4). This is in contrast to non-transgenic wild-type animals that bias their responses to low-intensity stimuli toward reorientation behaviors,[18] indicating that CaSR expression in neurons is both necessary and sufficient to bias sensorimotor

decision making. Second, computational analysis on larvae with variegated neuronal CaSR expression identified the DCR6 hindbrain neuronal cluster as a region where CaSR expression strongly correlates with decision-making outcomes (Figure 5). Third, driving CaSR expression in multiple other specific subsets of neurons in the brain failed to shift decision making in siblings or rescue mutants (Figure 3), while selectively targeting CaSR expression to the y234/DCR6 both shifted decision making in siblings and restored sensorimotor decision making in *CaSR* mutants (Figures 6B and 6E). Fourth, a subset of y234/DCR6 neurons project directly to the Mauthner lateral dendrite (Figure 6F), a key site of sensory processing for acoustically evoked escape initiation. Taken together these results provide compelling evidence that the y234/DCR6 is a key brain region for CaSR-dependent regulation of the bias between escape and reorientation behaviors.

The role of CaSR in y234/DCR6 neurons

CaSR acts via specific G protein molecular signaling pathways, and we previously identified two signaling pathways downstream of CaSR that regulate decision making: G$\alpha_{i/o}$ and G$\alpha_{q/11}$.[18] Identifying that CaSR acts in neurons to regulate decision making (Figure 2) makes it possible to focus on neuronal pathways that these downstream effectors regulate. The Gα_i effector reduces excitability in neurons via multiple mechanisms. Gα_i activation inhibits the activity of adenylate cyclase, therefore decreasing cAMP concentration, while also activating G-protein-gated inwardly rectifying potassium channels and inhibiting voltage-gated calcium channels.[69] Additionally, the G$\alpha_{q/11}$ pathway activates the phospholipase C pathway, which in turn generates inositol triphosphate (IP$_3$) and diacylglycerol (DAG), leading to the release of calcium from intracellular
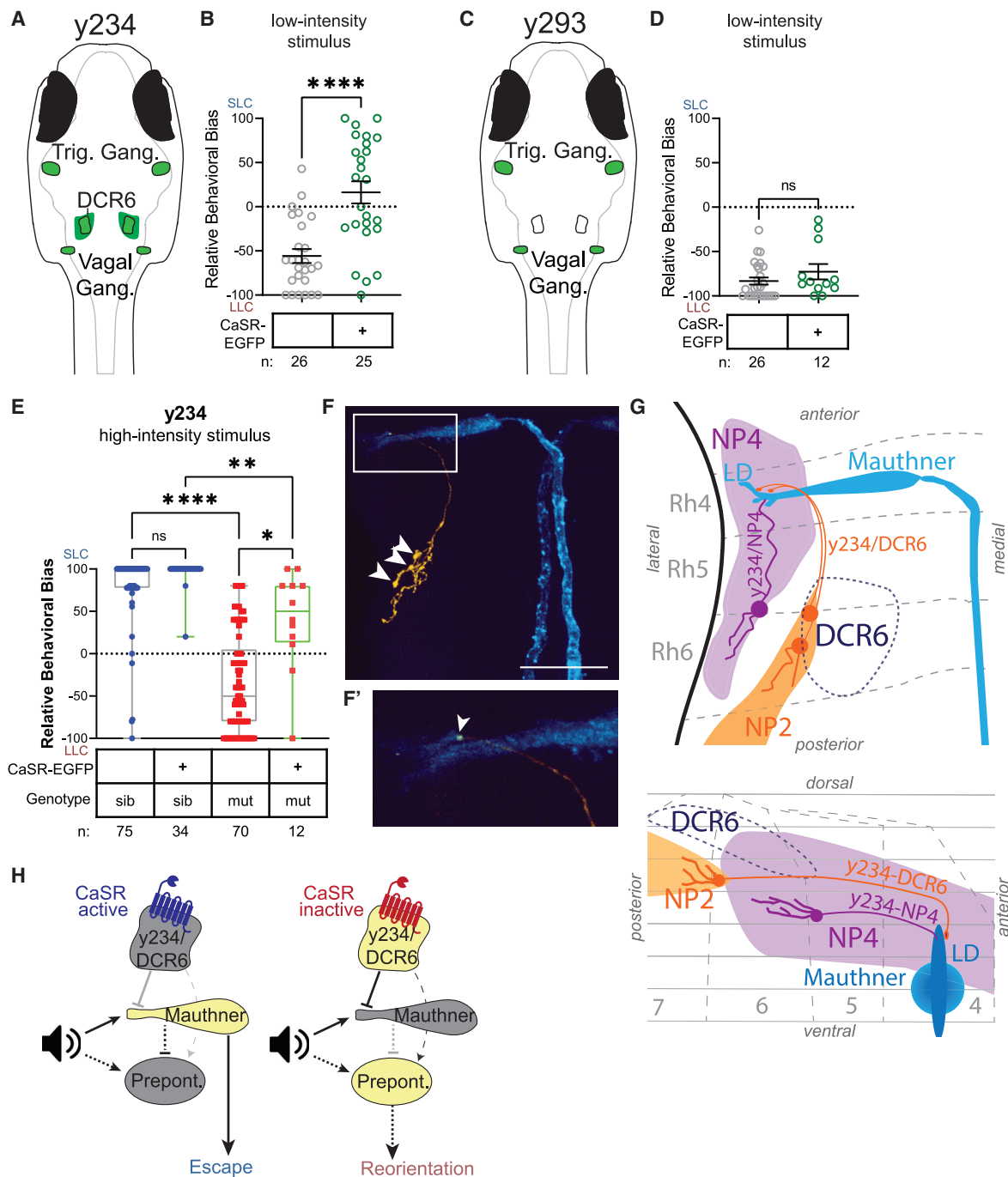
Figure 6. The y234/DCR6 is a key site for CaSR-dependent decision making

(A) Cartoon of trigeminal ganglion, vagal ganglion, and DCR6 expression driven by the *y234:Gal4* line. All expression patterns are based on images from ZBrain 2.0 brain browser; trigeminal ganglion from slice 35, vagal ganglion from slice 40, and Rhombencephalon QRFP Cluster Sparse (DCR6) from slice 120.

(B) Relative behavioral bias in response to weak stimuli of larvae generated by crossing *Et(y234:Gal4)* x *Tg(UAS:CaSR-EGFP); CaSR$^{p190/+}$* adults. p < 0.0001, Mann-Whitney U test. Lines represent means +/− SEM.

(C) Cartoon of trigeminal and vagal ganglion expression driven by the *y293:Gal4* line.

(D) Relative behavioral bias in response to weak stimuli of *CaSR* sibling larvae generated by crossing *Et(y293:Gal4); UAS:CaSR-EGFP; CaSR$^{p190/+}$* x *Tg(UAS:CaSR-EGFP); CaSR$^{p190/+}$* adults. p = 0.2234, Mann-Whitney U test. Lines represent means +/− SEM.

(E) Relative behavioral bias in response to strong stimuli of *CaSR* sibling and mutant larvae generated by crossing *Et(y234:Gal4); UAS:CaSR-EGFP; CaSR$^{p190/+}$* x *Tg(UAS:CaSR-EGFP); CaSR$^{p190/+}$* adults. p = 0.0392, mutants with vs. without CaSR-EGFP expression, Kruskal-Wallis with Dunn's post hoc test.

(legend continued on next page)

stores.[70] CaSR activates calcium-sensitive potassium (KCa) channels in neurons, likely via the increase of intracellular calcium, thereby hyperpolarizing the cell and reducing neuronal excitability.[71] Finally, neuronal CaSR activation can reduce currents through various different cation channels via unknown G protein effectors, which likely also dampens neuronal activity[32,72] and/or reduces the probability of vesicle release at the synapse.[73,74] It is therefore tempting to speculate that activating or overexpressing CaSR in y234/DCR6 neurons dampens their activity and/or synaptic release. Furthermore, downstream targets of CaSR in neurons, such as KCa channels, are promising molecular candidates for roles in decision making. Characterizing whether downstream targets of CaSR are expressed in and/or regulate decision making via the y234/DCR6 will further complete the picture of how CaSR regulates sensorimotor decision making. Although the relevant targets of CaSR signaling in y234/DCR6 neurons remain to be determined, our current data are consistent with the idea that reducing CaSR activity in the y234/DCR6 leads to overall greater neuronal activity in this region, while increasing CaSR activity reduces neuronal activity and y234/DCR6 output.

The role of y234/DCR6 neurons in sensorimotor decision making

Our results provide compelling evidence that, rather than the well-documented SLC or LLC circuitry, the hindbrain y234/DCR6 mediates CaSR-dependent sensorimotor decision making. Sensorimotor decision making consists of multiple steps, including sensory transduction, processing, and integration with internal state,[75] behavioral selection, and motor performance. Our previous work suggested that CaSR-dependent regulation of decision making occurs at or upstream of the Mauthner cell neuron.[18] Here, we provide compelling evidence that CaSR function is dispensable in populations that mediate sensory transduction (hair cells, Figure 2) and behavioral selection (Mauthner cell and prepontine neurons, Figure 3). Rather, CaSR might regulate sensory processing via the y234/DCR6 cluster and the Mauthner lateral dendrite. It is tempting to speculate that given their relatively caudal location in the hindbrain, y234/DCR6 neurons might integrate internal state information

such as ongoing behaviors to bias the activation of escape versus reorientation circuits.[17]

Consistent with this, we propose a model in which CaSR activity limits y234/DCR6 activity, which in turns limits Mauthner activity and hence the initiation of the escape behavior (Figure 6H). Thus, the most parsimonious model is that increasing CaSR activity in the y234/DCR6 increases the probability of escape behavior initiation and decreases the probability of the reorientation behavior, while reducing CaSR activity in the y234/DCR6 does the opposite. Despite our inability to detect axonal projections from the y234/DCR6 to prepontine neurons (Figure 6H), we cannot exclude the possibility that y234/DCR6 neurons directly or indirectly provide excitatory drive via to reorientation-mediating prepontine neurons. Mauthner activation temporally precedes activation of y293-prepontine neurons, so in the absence of Mauthner activation, the y293-prepontine neurons are freed from inhibition,[43] allowing them to initiate the reorientation behavior. Independent of the precise circuit mechanism by which CaSR regulates sensorimotor decision making and given the widespread responsiveness of hindbrain neurons to acoustic stimuli,[76,77] it is feasible that besides the y234/DCR6 neurons, additional hitherto unknown neuronal populations participate in sensory processing and integration critical for sensorimotor decision making. A critical next step will be to determine the connectivity, neurotransmitter identity, and pattern of neuronal activity of all neurons of the y234/DCR6 cluster. Combined with our current results, this will provide a more integrated understanding of how CaSR bidirectionally regulates the acute functioning of this decision-making circuit.

Limitations of the study

One potential limitation of our study is that the MAVEN method uses ZBrain atlas brain regions as its fundamental unit of analysis. Therefore, this method is less powered in its ability to identify roles for populations that do not directly correspond to defined brain regions in the atlas. A second, technical limitation is that our study identifies a critical decision-making population of neurons through a Gal4/UAS cell-specific rescue strategy, which is limited by the availability of specific Gal4 drivers.

(F) Maximum projection of *Et(y234:Gal4); Tg(hsp70GFF62a:Gal4); Tg(UAS:gap43-citrine)* larvae with sparse expression in the y234/DCR6. The Mauthner (blue) and y234/DCR6 neurons (orange) have been pseudocolored to allow clear visualization of the y234/DCR6 axon that projects dorsally and across the Mauthner lateral dendrite, where it eventually terminates. Three cell bodies in the y234/DCR6 are demarcated with white arrows. Scale bar represents 50 um. (F′) zoomed image of the pseudocolored Mauthner lateral dendrite (blue) with arrow demarcating a possible axon terminal bouton from y234/DCR6 neurons (orange).

(G) Top view and side view of the brain spanning from the DCR6 (most dorsal, purple outline) to the Mauthner neuron (most ventral, blue) including neuropil region 2 (NP2, orange), neuropil region 4 (NP4, magenta), and two projections to the Mauthner lateral dendrite labeled by *y234:Gal4*. The y234/DCR6 projection originates in neuropil 2, proximal to the ZBrain-defined DCR6, and was observed in 6/13 larvae in the sparse labeling experiment in (F), including the larva pictured in (F). The y234/NP4 projection originates in neuropil 4, lateral to the ZBrain-defined DCR6, and was observed in 4/13 larvae in the sparse labeling experiment in (F). Rhombomeres are labeled by number. Dashed lines in the lateral view indicate approximately 10-μm increments. All anatomy is based on the ZBrain 2.0 atlas and sparse labeling experiments.

(H) Proposed model of how CaSR signaling in the y234/DCR6 modulates the escape versus reorientation decision-making circuit. Yellow, more active brain region/neuron. Gray, less active brain region/neuron/synapse. Dashed lines indicate indirect or uncharacterized synaptic connections. T bars indicate inhibitory connections. Left: when CaSR activity in the y234/DCR6 is high, y234/DCR6 activity is high. High DCR6 activity dampens Mauthner activity, freeing prepontine neurons from inhibition and resulting in reorientation behaviors. The y234/DCR6 may also excite prepontine reorientation-mediating neurons, although we did not identify a projection from the y234/DCR6 to the prepontine region. Right: when CaSR activity in the y234/DCR6 is high, y234/DCR6 activity is low. Low y234/DCR6 activity frees the Mauthner lateral dendrite from inhibition, allowing the Mauthner to initiate escapes while simultaneously inhibiting initiation of the less-prioritized behavior, reorientations. Right: when CaSR activity in the y234/DCR6 is low, y234/DCR6 activity is high. High y234/DCR6 activity dampens Mauthner lateral dendrite activation by acoustic stimuli, freeing prepontine neurons from inhibition and resulting in reorientation behaviors.

Specifically, failure to rescue the *CaSR* mutant phenotype through expression in other neuronal populations does not exclude the possibility that CaSR might at least partially act in these populations, mainly because CaSR expression levels using Gal4 drivers might be too low or too mosaic to restore CaSR function. Despite these limitations, our findings nevertheless identify that the genetically defined y234/DCR6 hindbrain region mediates sensorimotor decision making via the vertebrate-specific G-protein-coupled receptor CaSR.

STAR★METHODS

Detailed methods are provided in the online version of this paper and include the following:

- KEY RESOURCES TABLE
- RESOURCE AVAILABILITY
  - Lead contact
  - Materials availability
  - Data and code availability
- EXPERIMENTAL MODEL AND SUBJECT DETAILS
  - Fish maintenance
- METHOD DETAILS
  - Behavioral testing and analysis
  - Cloning of transgenes and transgenic line creation
  - Mutant genotyping
  - Heat shock experiments
  - Cell type-specific rescue experiments
  - Dose-dependent rescue strength analysis
  - Imaging y234 neurons
  - Multivariate Analysis of Variegated Expression in Neurons (MAVEN)
- QUANTIFICATION AND STATISTICAL ANALYSIS

AUTHOR CONTRIBUTIONS

H.S.: conceptualization, formal analysis, funding acquisition, investigation, resources, software, visualization, writing – original draft, writing – review and editing. R.J.: conceptualization, resources, writing – review and editing. M.G.: conceptualization, funding acquisition, project administration, supervision, writing – original draft, writing – review and editing.

REFERENCES

1. von Reyn, C.R., Breads, P., Peek, M.Y., Zheng, G.Z., Williamson, W.R., Yee, A.L., Leonardo, A., and Card, G.M. (2014). A spike-timing mechanism for action selection. Nat. Neurosci. *17*, 962–970.

2. von Reyn, C.R., Nern, A., Williamson, W.R., Breads, P., Wu, M., Namiki, S., and Card, G.M. (2017). Feature integration drives probabilistic behavior in the Drosophila escape response. Neuron *94*, 1190–1204.e6.

3. International Brain Laboratory; Aguillon-Rodriguez, V., Angelaki, D., Bayer, H., Bonacchi, N., Carandini, M., Cazettes, F., Chapuis, G., Churchland, A.K., Dan, Y., et al. (2021). Standardized and reproducible measurement of decision-making in mice. Elife *10*, e63711.

4. Flavell, S.W., Pokala, N., Macosko, E.Z., Albrecht, D.R., Larsch, J., and Bargmann, C.I. (2013). Serotonin and the neuropeptide PDF initiate and extend opposing behavioral states in C. elegans. Cell *154*, 1023–1035.

5. Ache, J.M., Namiki, S., Lee, A., Branson, K., and Card, G.M. (2019). State-dependent decoupling of sensory and motor circuits underlies behavioral flexibility in Drosophila. Nat. Neurosci. *22*, 1132–1139.

6. Ghosh, D.D., Sanders, T., Hong, S., McCurdy, L.Y., Chase, D.L., Cohen, N., Koelle, M.R., and Nitabach, M.N. (2016). Neural architecture of hunger-dependent multisensory decision making in C. elegans. Neuron *92*, 1049–1062.

7. Filosa, A., Barker, A.J., Dal Maschio, M., and Baier, H. (2016). Feeding state modulates behavioral choice and processing of prey stimuli in the zebrafish tectum. Neuron *90*, 596–608. https://doi.org/10.1016/j.neuron.2016.03.014.

8. Barker, A.J., and Baier, H. (2015). Sensorimotor decision making in the zebrafish tectum. Curr. Biol. *25*, 2804–2814.

9. Jovanic, T., Schneider-Mizell, C.M., Shao, M., Masson, J.B., Denisov, G., Fetter, R.D., Mensh, B.D., Truman, J.W., Cardona, A., and Zlatic, M. (2016). Competitive disinhibition mediates behavioral choice and sequences in Drosophila. Cell *167*, 858–870.e19.

10. Calhoun, A.J., Pillow, J.W., and Murthy, M. (2019). Unsupervised identification of the internal states that shape natural behavior. Nat. Neurosci. *22*, 2040–2049.

11. McIntyre, C., and Preuss, T. (2019). Influence of stimulus intensity on multimodal integration in the startle escape system of goldfish. Front. Neural Circ. *13*, 7.

12. Yang, H., Kwon, S.E., Severson, K.S., and O'Connor, D.H. (2015). Origins of choice-related activity in mouse somatosensory cortex. Nat. Neurosci. *19*, 127–134.

13. MacOsko, E.Z., Pokala, N., Feinberg, E.H., Chalasani, S.H., Butcher, R.A., Clardy, J., and Bargmann, C.I. (2009). A hub-and-spoke circuit drives pheromone attraction and social behaviour in C. elegans. Nature *458*, 1171–1175.

14. Kalueff, A.V., Olivier, J.D.A., Nonkes, L.J.P., and Homberg, J.R. (2010). Conserved role for the serotonin transporter gene in rat and mouse neurobehavioral endophenotypes. Neurosci. Biobehav. Rev. *34*, 373–386.

15. Jang, H., Kim, K., Neal, S.J., Macosko, E., Kim, D., Butcher, R.A., Zeiger, D.M., Bargmann, C.I., and Sengupta, P. (2012). Neuromodulatory state and sex specify alternative behaviors through antagonistic synaptic pathways in C. elegans. Neuron *75*, 585–592.

16. Seeholzer, L.F., Seppo, M., Stern, D.L., and Ruta, V. (2018). Evolution of a central neural circuit underlies Drosophila mate preferences. Nature *559*, 564–569.

17. Burgess, H.A., and Granato, M. (2007). Sensorimotor gating in larval zebrafish. J. Neurosci. *27*, 4984–4994.

18. Jain, R.A., Wolman, M.A., Marsden, K.C., Nelson, J.C., Shoenhard, H., Echeverry, F.A., Szi, C., Bell, H., Skinner, J., Cobbs, E.N., et al. (2018). A forward genetic screen in zebrafish identifies the G-protein coupled receptor CaSR as a regulator of sensorimotor decision-making. Curr. Biol. *28*, 1357–1369.e5.

19. Brown, E.M., Gamba, G., Riccardi, D., Lombardi, M., Butters, R., Kifor, O., Sun, A., Hediger, M.A., Lytton, J., and Hebert, S.C. (1993). Cloning and characterization of an extracellular Ca(2+)-sensing receptor from bovine parathyroid. Nature 366, 575–580.

20. Herberger, A.L., and Loretz, C.A. (2013). Vertebrate extracellular calcium-sensing receptor evolution: selection in relation to life history and habitat. Comp. Biochem. Physiol., Part D: Genomics Proteomics 8, 86–94.

21. Hannan, F.M., Kallay, E., Chang, W., Brandi, M.L., and Thakker, R.V. (2018). The calcium-sensing receptor in physiology and in calcitropic and noncalcitropic diseases. Nat. Rev. Endocrinol. 15, 33–51.

22. Kwong, R.W.M., Auprix, D., and Perry, S.F. (2014). Involvement of the calcium-sensing receptor in calcium homeostasis in larval zebrafish exposed to low environmental calcium. Am. J. Physiol. Regul. Integr. Comp. Physiol. 306, R211–R221.

23. Lin, C.-H., Su, C.-H., and Hwang, P.-P. (2014). Calcium-sensing receptor mediates Ca(2+) homeostasis by modulating expression of PTH and stanniocalcin. Endocrinology 155, 56–67.

24. Mateo-Lozano, S., García, M., Rodríguez-Hernández, C.J., and de Torres, C. (2016). Regulation of differentiation by calcium-sensing receptor in normal and tumoral developing nervous system. Front. Physiol. 7, 169.

25. Vizard, T.N., O'Keeffe, G.W., Gutierrez, H., Kos, C.H., Riccardi, D., and Davies, A.M. (2008). Regulation of axonal and dendritic growth by the extracellular calcium-sensing receptor. Nat. Neurosci. 11, 285–291.

26. Vizard, T.N., Newton, M., Howard, L., Wyatt, S., and Davies, A.M. (2015). ERK signaling mediates CaSR-promoted axon growth. Neurosci. Lett. 603, 77–83.

27. Markworth, R., Adolfs, Y., Dambeck, V., Steinbeck, L.M., Lizé, M., Pasterkamp, R.J., Bähr, M., Dean, C., and Burk, K. (2019). Sensory axon growth requires spatiotemporal integration of CaSR and TrkB signaling. J. Neurosci. 39, 5842–5860.

28. Ruat, M., and Traiffort, E. (2013). Roles of the calcium sensing receptor in the central nervous system. Best Pract. Res. Clin. Endocrinol. Metab. 27, 429–442.

29. Giudice, M.L., Mihalik, B., Dinnyés, A., and Kobolák, J. (2019). The nervous system relevance of the calcium sensing receptor in health and disease. Molecules 24, E2546.

30. Dal Pra, I., Chiarini, A., Nemeth, E.F., Armato, U., and Whitfield, J.F. (2005). Roles of Ca2+ and the Ca2+-sensing receptor (CASR) in the expression of inducible NOS (nitric oxide synthase)-2 and its BH4 (tetrahydrobiopterin)-dependent activation in cytokine-stimulated adult human astrocytes. J. Cell. Biochem. 96, 428–438.

31. Chen, W., Bergsman, J.B., Wang, X., Gilkey, G., Pierpoint, C.R., Daniel, E.A., Awumey, E.M., Dauban, P., Dodd, R.H., Ruat, M., and Smith, S.M. (2010). Presynaptic external calcium signaling Involves the calcium-sensing receptor in neocortical nerve terminals. PLoS One 5, e8563.

32. Lu, B., Zhang, Q., Wang, H., Wang, Y., Nakayama, M., and Ren, D. (2010). Extracellular calcium controls background current and neuronal excitability via an UNC79-UNC80-NALCN cation channel complex. Neuron 68, 488–499.

33. Jones, B.L., and Smith, S.M. (2016). Calcium-sensing receptor: a key target for extracellular calcium signaling in neurons. Front. Physiol. 7, 116.

34. Chattopadhyay, N., Espinosa-Jeffrey, A., Tfelt-Hansen, J., Yano, S., Bandyopadhyay, S., Brown, E.M., and de Vellis, J. (2008). Calcium receptor expression and function in oligodendrocyte commitment and lineage progression: potential impact on reduced myelin basic protein in CaR-null mice. J. Neurosci. Res. 86, 2159–2167.

35. Eaton, R.C., Farley, R.D., Kimmel, C.B., and Schabtach, E. (1977). Functional development in the mauthner cell system of embryos and larvae of the zebra fish. J. Neurobiol. 8, 151–172.

36. Lin, L.-Y., Yeh, Y.H., Hung, G.Y., Lin, C.H., Hwang, P.P., and Horng, J.L. (2018). Role of calcium-sensing receptor in mechanotransducer-channel-mediated Ca2+ influx in hair cells of zebrafish larvae. Front. Physiol. 9, 649.

37. Scheer, N., and Campos-Ortega, J.A. (1999). Use of the Gal4-UAS technique for targeted gene expression in the zebrafish. Mech. Dev. 80, 153–158.

38. Kimmel, C.B., Eaton, R.C., and Powell, S.L. (1980). Decreased fast-start performance of zebrafish larvae lacking mauthner neurons. J. Comp. Physiol. 140, 343–350.

39. Liu, K.S., and Fetcho, J.R. (1999). Laser ablations reveal functional relationships of segmental hindbrain neurons in zebrafish. Neuron 23, 325–335.

40. Hale, M.E., Kheirbek, M.A., Schriefer, J.E., and Prince, V.E. (2004). Hox gene misexpression and cell-specific lesions reveal functionality of homeotically transformed neurons. J. Neurosci. 24, 3070–3076.

41. Lacoste, A.M.B., Schoppik, D., Robson, D.N., Haesemeyer, M., Portugues, R., Li, J.M., Randlett, O., Wee, C.L., Engert, F., and Schier, A.F. (2015). A convergent and essential interneuron pathway for Mauthner-cell-mediated escapes. Curr. Biol. 25, 1526–1534.

42. Hecker, A., Schulze, W., Oster, J., Richter, D.O., and Schuster, S. (2020). Removing a single neuron in a vertebrate brain forever abolishes an essential behavior. Proc. Natl. Acad. Sci. USA 117, 3254–3260.

43. Marquart, G.D., Tabor, K.M., Bergeron, S.A., Briggman, K.L., and Burgess, H.A. (2019). Prepontine non-giant neurons drive flexible escape behavior in zebrafish. PLoS Biol. 17, e3000480.

44. Pujol-Martí, J., Zecca, A., Baudoin, J.P., Faucherre, A., Asakawa, K., Kawakami, K., and López-Schier, H. (2012). Neuronal birth order identifies a dimorphic sensorineural map. J. Neurosci. 32, 2976–2987.

45. Satou, C., Kimura, Y., Hirata, H., Suster, M.L., Kawakami, K., and Higashijima, S.i. (2013). Transgenic tools to characterize neuronal properties of discrete populations of zebrafish neurons. Development 140, 3927–3931.

46. Koyama, M., Kinkhabwala, A., Satou, C., Higashijima, S.i., and Fetcho, J. (2011). Mapping a sensory-motor network onto a structural and functional ground plan in the hindbrain. Proc. Natl. Acad. Sci. USA 108, 1170–1175.

47. Marques, J.C., Li, M., Schaak, D., Robson, D.N., and Li, J.M. (2019). Internal state dynamics shape brainwide activity and foraging behaviour. Nature 577, 239–243.

48. Ohmura, Y., Iwami, K., Chowdhury, S., Sasamori, H., Sugiura, C., Bouchekioua, Y., Nishitani, N., Yamanaka, A., and Yoshioka, M. (2021). Disruption of model-based decision making by silencing of serotonin neurons in the dorsal raphe nucleus. Curr. Biol. 31, 2446–2454.e5.

49. Xing, L., Son, J.H., Stevenson, T.J., Lillesaar, C., Bally-Cuif, L., Dahl, T., and Bonkowsky, J.L. (2015). A serotonin circuit acts as an environmental sensor to mediate midline axon crossing through EphrinB2. J. Neurosci. 35, 14794–14808.

50. Akitake, C.M., Macurak, M., Halpern, M.E., and Goll, M.G. (2011). Transgenerational analysis of transcriptional silencing in zebrafish. Dev. Biol. 352, 191–201.

51. Goll, M.G., Anderson, R., Stainier, D.Y.R., Spradling, A.C., and Halpern, M.E. (2009). Transcriptional silencing and reactivation in transgenic zebrafish. Genetics 182, 747–755.

52. Randlett, O., Wee, C.L., Naumann, E.A., Nnaemeka, O., Schoppik, D., Fitzgerald, J.E., Portugues, R., Lacoste, A.M.B., Riegler, C., Engert, F., and Schier, A.F. (2015). Whole-brain activity mapping onto a zebrafish brain atlas. Nat. Methods 12, 1039–1046.

53. Tibshirani, R. (1996). Regression shrinkage and selection via the Lasso. J. Roy. Stat. Soc. B 58, 267–288.

54. Shainer, I., Kuehn, E., Laurell, E., Kassar, M.A., Mokayes, N., Sherman, S., Larsch, J., Kunst, M., and Baier, H. (2022). A single-cell resolution gene expression atlas of the larval zebrafish brain. Preprint at bioRxiv. https://doi.org/10.1101/2022.02.11.479024.

55. Yokogawa, T., Hannan, M.C., and Burgess, H.A. (2012). The dorsal raphe modulates sensory responsiveness during arousal in zebrafish. J. Neurosci. 32, 15205–15215.

56. Lakhina, V., Marcaccio, C.L., Shao, X., Lush, M.E., Jain, R.A., Fujimoto, E., Bonkowsky, J.L., Granato, M., and Raper, J.A. (2012). Netrin/DCC

signaling guides olfactory sensory axons to their correct location in the olfactory bulb. J. Neurosci. *32*, 4440–4456.

57. Yamanaka, I., Miki, M., Asakawa, K., Kawakami, K., Oda, Y., and Hirata, H. (2013). Glycinergic transmission and postsynaptic activation of CaMKII are required for glycine receptor clustering in vivo. Gene Cell. *18*, 211–224.

58. Yao, C., Vanderpool, K.G., Delfiner, M., Eddy, V., Lucaci, A.G., Soto-Riveros, C., Yasumura, T., Rash, J.E., and Pereda, A.E. (2014). Electrical synaptic transmission in developing zebrafish: properties and molecular composition of gap junctions at a central auditory synapse. J. Neurophysiol. *112*, 2102–2113.

59. Marsden, K.C., and Granato, M. (2015). In vivo Ca2+ imaging reveals that decreased dendritic excitability drives startle habituation. Cell Rep. *13*, 1733–1740.

60. Pantoja, C., Hoagland, A., Carroll, E.C., Karalis, V., Conner, A., and Isacoff, E.Y. (2016). Neuromodulatory regulation of behavioral individuality in zebrafish. Neuron *91*, 587–601.

61. Shohamy, D., and Daw, N.D. (2015). Integrating memories to guide decisions. Curr. Opin. Behav. Sci. *5*, 85–90.

62. Lloyd, K., and Dayan, P. (2018). Interrupting behaviour: minimizing decision costs via temporal commitment and low-level interrupts. PLoS Comput. Biol. *14*, e1005916.

63. Evans, D.A., Stempel, A.V., Vale, R., and Branco, T. (2019). Cognitive control of escape behaviour. Trends Cogn. Sci. *23*, 334–348.

64. Chen, C.-L., Aymanns, F., Minegishi, R., Matsuda, V., Talabot, N., Gunel, S., Dickson, B.J., and Ramdya, P. (2022). Ascending neurons convey behavioral state to integrative sensory and action selection centers in the brain. Preprint at bioRxiv. https://doi.org/10.1101/2022.02.09.479566.

65. Hindmarsh Sten, T., Li, R., Otopalik, A., and Ruta, V. (2021). Sexual arousal gates visual processing during Drosophila courtship. Nature *595*, 549–553.

66. Ashwood, Z.C., Roy, N.A., Stone, I.R., International Brain Laboratory; Urai, A.E., Churchland, A.K., Pouget, A., and Pillow, J.W. (2022). Mice alternate between discrete strategies during perceptual decision-making. Nat. Neurosci. *25*, 201–212.

67. Long, A.B., Kuhn, C.M., and Platt, M.L. (2009). Serotonin shapes risky decision making in monkeys. Soc. Cogn. Affect. Neurosci. *4*, 346–356.

68. Schultz, W. (2015). Neuronal reward and decision signals: from theories to data. Physiol. Rev. *95*, 853–951.

69. Yudin, Y., and Rohacs, T. (2018). Inhibitory G i/O-coupled receptors in somatosensory neurons: potential therapeutic targets for novel analgesics. Mol. Pain *14*. 1744806918763646.

70. Kifor, O., MacLeod, R.J., Diaz, R., Bai, M., Yamaguchi, T., Yao, T., Kifor, I., and Brown, E.M. (2001). Regulation of MAP kinase by calcium-sensing receptor in bovine parathyroid and CaR-transfected HEK293 cells. Am. J. Physiol. Renal Physiol. *280*, F291–F302.

71. Vassilev, P.M., Ho-Pao, C.L., Kanazirska, M.P., Ye, C., Hong, K., Seidman, C.E., Seidman, J.G., and Brown, E.M. (1997). Cao-sensing receptor (CaR)-mediated activation of K+ channels is blunted in CaR gene-deficient mouse neurons. Neuroreport *8*, 1411–1416.

72. Martiszus, B.J., Tsintsadze, T., Chang, W., and Smith, S.M. (2021). Enhanced excitability of cortical neurons in low-divalent solutions is primarily mediated by altered voltage-dependence of voltage-gated sodium channels. Elife *10*, e67914.

73. Phillips, C.G., Harnett, M.T., Chen, W., and Smith, S.M. (2008). Calcium-sensing receptor activation depresses synaptic transmission. J. Neurosci. *28*, 12062–12070.

74. O'Seaghdha, C.M., Yang, Q., Glazer, N.L., Leak, T.S., Dehghan, A., Smith, A.V., Kao, W.H.L., Lohman, K., Hwang, S.J., Johnson, A.D., et al. (2010). Common variants in the calcium-sensing receptor gene are associated with total serum calcium levels. Hum. Mol. Genet. *19*, 4296–4303.

75. Kristan, W.B. (2008). Neuronal decision-making circuits. Curr. Biol. *18*, R928–R932.

76. Gahtan, E., Sankrithi, N., Campos, J.B., and O'Malley, D.M. (2002). Evidence for a widespread brain stem escape network in larval zebrafish. J. Neurophysiol. *87*, 608–614.

77. Privat, M., Romano, S.A., Pietri, T., Jouary, A., Boulanger-Weill, J., Elbaz, N., Duchemin, A., Soares, D., and Sumbre, G. (2019). Sensorimotor transformations in the zebrafish auditory system. Curr. Biol. *29*, 4010–4023.e4.

78. Leung, L.C., Wang, G.X., Madelaine, R., Skariah, G., Kawakami, K., Deisseroth, K., Urban, A.E., and Mourrain, P. (2019). Neural signatures of sleep in zebrafish. Nature *571*, 198–204.

79. Kwan, K.M., Fujimoto, E., Grabher, C., Mangum, B.D., Hardy, M.E., Campbell, D.S., Parant, J.M., Yost, H.J., Kanki, J.P., and Chien, C.B. (2007). The Tol2kit: a multisite gateway-based construction kit for Tol2 transposon transgenesis constructs. Dev. Dyn. *236*, 3088–3099.

80. Kindt, K.S., Finch, G., and Nicolson, T. (2012). Kinocilia mediate mechanosensitivity in developing zebrafish hair cells. Dev. Cell *23*, 329–341.

81. Don, E.K., Formella, I., Badrock, A.P., Hall, T.E., Morsch, M., Hortle, E., Hogan, A., Chow, S., Gwee, S.S.L., Stoddart, J.J., et al. (2017). A Tol2 gateway-compatible toolbox for the study of the nervous system and neurodegenerative disease. Zebrafish *14*, 69–72.

82. Berger, J., and Currie, P.D. (2013). A small and muscle-specific zebrafish promoter. Genesis *51*, 443–447.

83. Wolman, M.A., Jain, R.A., Marsden, K.C., Bell, H., Skinner, J., Hayer, K.E., Hogenesch, J.B., and Granato, M. (2015). A genome-wide screen identifies PAPP-AA-Mediated IGFR signaling as a novel regulator of habituation learning. Neuron *85*, 1200–1211.

84. Wolman, M.A., Jain, R.A., Liss, L., and Granato, M. (2011). Chemical modulation of memory formation in larval zebrafish. Proc. Natl. Acad. Sci. USA *108*, 15468–15473.

85. Suster, M.L., Kikuta, H., Urasaki, A., Asakawa, K., and Kawakami, K. (2009). Transgenesis in zebrafish with the tol2 transposon system. Methods Mol. Biol. *561*, 41–63.

86. Koga, A., Cheah, F.S.H., Hamaguchi, S., Yeo, G.H., and Chong, S.S. (2008). Germline transgenesis of zebrafish using the medaka Tol1 transposon system. Dev. Dyn. *237*, 2466–2474.

87. Meeker, N.D., Hutchinson, S.A., Ho, L., and Trede, N.S. (2007). Method for isolation of PCR-ready genomic DNA from zebrafish tissues. Biotechniques *43*, 610–614.

88. Hieber, V., Dai, X., Foreman, M., and Goldman, D. (1998). Induction of 1-tubulin gene expression during development and regeneration of the fish central nervous system. J. Neurobiol. *37*, 429–440.

89. Shimizu, Y., Ito, Y., Tanaka, H., and Ohshima, T. (2015). Radial glial cell-specific ablation in the adult Zebrafish brain. Genesis *53*, 431–439.

90. Lee, R.T.H., Knapik, E.W., Thiery, J.P., and Carney, T.J. (2013). An exclusively mesodermal origin of fin mesenchyme demonstrates that zebrafish trunk neural crest does not generate ectomesenchyme. Development *140*, 2923–2932.

91. Preston, M.A., and Macklin, W.B. (2015). Zebrafish as a model to investigate CNS myelination. Glia *63*, 177–193.

92. Marquart, G.D., Tabor, K.M., Brown, M., Strykowski, J.L., Varshney, G.K., LaFave, M.C., Mueller, T., Burgess, S.M., Higashijima, S.I., and Burgess, H.A. (2015). A 3D searchable database of transgenic zebrafish Gal4 and Cre lines for functional neuroanatomy studies. Front. Neural Circ. *9*, 78.

STAR★METHODS

KEY RESOURCES TABLE

REAGENT or RESOURCE	SOURCE	IDENTIFIER
Antibodies		
mouse anti-tERK	Cell Signaling	RRID: AB_390780
chicken anti-GFP	Rockland	RRID: AB_1537404
goat anti-mouse	ThermoFisher Scientific	RRID: AB_2535768
donkey anti-chicken	Jackson ImmunoResearch Labs	RRID:AB_2340375
Bacterial and virus strains		
One-Shot TOP10 Chemically Competent Cells	Invitrogen	Cat# C404010
Experimental models: Organisms/strains		
zebrafish: *Tg(myo6b:CaSR-EGFP,cryaa:mCherry)*	This study	ZDB-ALT-220824-2
zebrafish: *Tg(UAS:CaSR-EGFP)*	This study	ZDB-ALT-220824-3
zebrafish: *Tg(hsp70:CaSR-EGFP,myl7:GFP)*	This study	ZDB-ALT-220824-4
zebrafish: *Tg(alpha-tubulin:Gal4,myl7:GFP)*	Leung et al. 2019[78]	ZDB-ALT-180816-20
zebrafish: *Tg(UAS:gap43-citrine)*	Lakhina et al. 2012[56]	ZDB-ALT-121206-2
zebrafish: *Et(y293:Gal4)*	Marquart et al. 2019[43]	ZDB-ALT-151216-1
zebrafish: *Et(y234:Gal4)*	Yokogawa, Hannan, and Burgess 2012[55]	ZDB-ALT-121114-10
zebrafish: *Et(GFFDMC130a)*	Pujol-Martí et al. 2012[44]	ZDB-ALT-120320-6
zebrafish: *Tg(Glyt2:Gal4,myl7:GFP)*	Satou et al. 2013[45]	ZDB-ALT-131127-3
zebrafish: *Tg(fev1:Gal4-GFP)*	Xing et al. 2015[49]	ZDB-ALT-160209-2
zebrafish: *Tg(-6.7FRhcrtR:gal4VP16)*	Lacoste et al. 2015[41]	ZFIN: ZDB-TGCONSTRCT-151028-8
zebrafish: *Tg(hspGFF62a:Gal4)*	Yamanaka et al. 2013[57]	ZDB-ALT-150717-1
zebrafish: *wrong turn/CaSR^p190*	Jain et al. 2018[18]	ZDB-ALT-171122-3
zebrafish: *CaSR^p198*	Jain et al. 2018[18]	ZDB-ALT-180117-4
Oligonucleotides		
Custom KASP primers made to genotype *CaSR^p190*, input sequence: ATTTTTTTCCAACTATTTCTCTTTTCT ACTGTCTCTCAGATTAGCTATGCTTCA[T/C] CCAGCCGCCTTTTGAGCAACA AAAACCAGTACAAATCCTTCATGAGG ACAATCCCT	LGC Genomics	N/A
Custom KASP primers made to genotype *CaSR^p198*, input sequence: CACTTCTTGCTTTCTGAAGCAAATCG AGTTTCTGTCCTGGACCGAACCGTTC GGGATTGCGCTGGCCTTATTTGC[AG TCCTC/-]GGGGTTCTCCTAACAGCTT TTGTGTTGGGTGTTTTTGTGCAATTC CGTGATACTCCAATCGTGAAGGCATC AAAC	LGC Genomics	N/A
Recombinant DNA		
pENTR CaSR-EGFP	This study	AddGene #191503
pTol1-14xUAS:CaSR-EGFP	This study	AddGene #191502
pTol2-hsp70:CaSR-EGFP, myl7:GFP	This study	AddGene #191501
pDestTol2CG2	Kwan et al. 2007[79]	–
pTol2-myo6b:CaSR-EGFP,cryaa:mCherry	This study	AddGene #191500
p5e myo6b	Kindt, Finch, and Nicolson 2012[80]	Provided by Kindt lab

(Continued on next page)

Continued

REAGENT or RESOURCE	SOURCE	IDENTIFIER
p3e MCS	Don et al. 2017[81]	AddGene # 75174
pTol1-14xUAS:NTR-TagRFPT	Harry Burgess lab	Provided by Burgess lab
pDESTtol2pACrymCherry	Berger and Currie 2013[82]	AddGene #64023
Software and algorithms		
R	The R Project for Statistical Computing	RRID:SCR_001905
RStudio	RStudio	RRID:SCR_000432
MATLAB	MathWorks	RRID:SCR_001622
FIJI ImageJ	GNU Open Source Software	RRID:SCR_002285
GraphPad Prism	Dotmatics	RRID:SCR_002798
SnapGene	Dotmatics	RRID:SCR_015052

RESOURCE AVAILABILITY

Lead contact

Further information and requests for reagents and resource may be directed to and will be fulfilled by the Lead Contact, Dr. Michael Granato (granatom@pennmedicine.upenn.edu).

Materials availability

Plasmids generated during this study have been deposited to Addgene (see key resources table). Transgenic zebrafish lines have been added to the ZFIN database (see key resources table). Requests for transgenic zebrafish should be directed to the lead contact.

Data and code availability

No datasets of standardized datatypes were generated for this study.

Custom MATLAB and R code generated for this study are available.

Any additional information required to reanalyze the data reported in this paper is available from the lead contact upon request.

EXPERIMENTAL MODEL AND SUBJECT DETAILS

Fish maintenance

All experiments with *Danio rerio* were approved by the University of Pennsylvania IACUC (protocol numbers 805167 and 805,140). $CaSR^{p190}$ and $CaSR^{p198}$ mutations were maintained in the wild-type Tübingen long fin (TLF) strain background. Embryos were raised in E3 at 28-29°C on a 14 h light/10 h dark cycle. All experiments were performed on 5 dpf larvae unless otherwise indicated. At this stage of development, zebrafish larvae sex is not determined, so we did not compare males and females.

Wild-type TLF larvae were assayed for decision making behavior every generation before being raised. Only clutches with typically wild-type behavioral bias—namely, strong bias toward SLCs in response to intense acoustic stimuli—were included in the assortment of wild-type larvae to be raised.

Et(y293:Gal4)[43] and *Et(y234:Gal4)*[55] fish were kindly provided by the lab of Harold Burgess. *Tg(alpha-tubulin:Gal4,myl7:GFP)*[78] fish were kindly provided by the lab of Phillipe Mourrain. *Tg(fev1:Gal4-GFP)* fish[49] were kindly provided by Christina Lillesaar.

METHOD DETAILS

Behavioral testing and analysis

All behavioral assays were performed during the day. To evoke a high proportion of SLCs in wild-type larvae, an 1100 Hz vibrational (acoustic) stimulus at 35.1 dB was applied to d5 or d6 larvae in a custom behavioral rig as previously described,[83] with an expanded grid for 36 larvae. This stimulus was repeated 10 times with an interstimulus interval of 20 s.[18] To evoke a high proportion of LLCs in wild-type larvae, a 1500 Hz vibrational (acoustic) stimulus at 25.5 dB was applied. This stimulus was repeated 30 times with an interstimulus interval of 20 s, because larvae were less responsive at this lower intensity and ≥ 4 responses are necessary to accurately compute relative behavioral bias (RBB). RBB is defined as (200 * (percent of stimuli reacted to with SLCs)/(percent of stimuli reacted to overall)) −100. When calculating RBB, larvae with <4 responses were filtered out the analysis. All tracking and analysis was performed using the FLOTE software platform.[17,84]

Cloning of transgenes and transgenic line creation

The *pTol2-myo6b:CaSR-EGFP,cryaa:mCherry* construct was generated by Gateway LR cloning (ThermoFisher) *p5e myo6b*,[80] *pENTR CaSR-EGFP*, and *p3e MCS* (AddGene # 75174[81]) into the destination vector *pDESTtol2pACrymCherry* (AddGene # 64023[82]) vector. DNA was midiprepped, phenol-chloroform extracted, and microinjected into one cell stage zebrafish embryos. Tol2 transgenesis was performed by microinjecting Tol2 mRNA and plasmid DNA as previously described.[85] *pTol2-hsp70:CaSR-EGFP,myl7:GFP* was created by using Gateway cloning to insert *p5e hsp70* and *pENTR CaSR-EGFP* into the *pDestTol2CG2* backbone.[79] *CaSR-EGFP* was cloned into the *pTol1-14xUAS:NTR-TagRFPT* backbone using the In-Fusion HD Cloning Plus Kit (Takara Biosciences) to create *pTol1-14xUAS:CaSR-EGFP*. *pTol1-14xUAS:CaSR-EGFP* was microinjected into *CaSR^{p190/+}* x TLF one cell stage larvae by microinjecting Tol1 mRNA and plasmid DNA as previously described.[86] Founders were identified by crossing injected g0 fish to *GlyT2:Gal4,myl7:GFP*[45] fish and screening for GFP expression in the brain.

Mutant genotyping

All behavioral experiments were performed blind to genotype, and all behavioral comparisons were made between siblings from the same experiment. Larvae to be genotyped were stored in methanol and lysed with the HotShot protocol. Methanol was allowed to evaporate off, then larvae were immersed in 50 mM NaOH, heated to 95°C for 15 min, then neutralized with 1M Tris-HCl.[87] *CaSR^{p190}* and *CaSR^{p198}* fish were genotyped using the KASP method with proprietary primer sequences (LGC Genomics). The *CaSR^{p190}* primers amplify only genomic CaSR, meaning they can be used to distinguish genomic *CaSR* mutants from siblings even in the context of transgenes containing *CaSR* cDNA.

Heat shock experiments

Tg(hsp70:CaSR-EGFP,myl7:GFP); CaSR^{p190/+} f1 were crossed to *CaSR^{p190/+}* fish to yield larvae that were sorted for green hearts at 2 dpf. Half of each group (heart+ and heart-) was heat shocked and half served as a negative control. For heat shock, larvae were placed in a 50 mL conical vial with pre-warmed E3, then incubated in a 37°C water bath for 45 min. Alternatively, larvae were placed in a thermocycler and incubated at 37°C for 45 min. Fluorescence in heat shocked *Tg(hsp70:CaSR-EGFP,myl7:GFP)* larvae was visually verified on an epifluorescent microscope without anesthetizing the larvae approximately one hour before behavioral testing.

Cell type-specific rescue experiments

We used the *Tg(myo6b:CaSR-EGFP,cryaa:mCherry)* direct promoter fusion line to drive CaSR expression in hair cells. Larvae were sorted on a fluorescent microscope using the red marker in the lens of the eye.

For Gal4 x UAS rescue experiments, *Tg(UAS:CaSR-EGFP); CaSR^{p190/+}* or *Tg(UAS:CaSR-EGFP); CaSR^{p198/+}* fish were crossed to Gal4 lines and offspring sorted for expected expression patterns, raised, and genotyped for CaSR, resulting in Gal4; *Tg(UAS:CaSR-EGFP); CaSR^{+/−}* fish. These fish were then incrossed and sorted for strong green fluorescent larvae (excluding larvae with visibly weak or mosaic expression) at 2–4 dpf using an Olympus SZX16 fluorescent microscope. Behavioral testing was performed at 5 dpf.

Note that due to genetic background effects from different Gal4 driver lines, the decision making bias of control larvae differs between groups. For this reason, the bias of larvae expressing versus not expressing transgenic CaSR should be compared within each background-matched cell type assayed, rather than comparing larvae of different genetic backgrounds to each other.

We crossed *Tg(UAS:CaSR-EGFP)* fish to the *Tg(alpha-tubulin:Gal4,myl7:GFP)* line to label neurons[78,88]; to the *Tg(gfap:Gal4)* line[89] to label radial astrocytes; and to the *Tg(sox10:Gal4)* line[90] to label neural crest cells, which include oligodendrocyte precursor cells (OPCs) and mature oligodendrocytes.[91]

We used the *Et(GFFDMC130a)* Gal4 line[44] to drive expression in the Mauthner neuron; the *Tg(-6.7FRhcrtR:gal4VP16)* line to drive expression in feedforward excitatory spiral fiber neurons;[41] and the *Tg(Glyt2:Gal4,myl7:GFP)* line to drive expression in glycinergic inhibitory neurons.[45] To drive expression in LLC-mediating neurons, we employed the *Et(y293:Gal4)* line[43,92] We used the *Tg(fev:Gal4-GFP)* line[49] to drive CaSR-EGFP expression in serotonergic neurons of the raphe nucleus. Because in this case the Gal4 was also labeled with GFP, we crossed a Gal4 carrier to a UAS carrier with two copies of the UAS construct so that all green + larvae must also be CaSR-EGFP+.

For y234/DCR6 overexpression experiments, we crossed *Et(y234:Gal4)*[55] x *Tg(UAS:CaSR-EGFP); CaSR^{p190/+}* adults, and *Et(y293:Gal4)*[43]; *UAS:CaSR-EGFP; CaSR^{p190/+}* x *Tg(UAS:CaSR-EGFP); CaSR^{p190/+}* adults. For y234/DCR6 rescue experiments, we crossed *Et(y234:Gal4); UAS:CaSR-EGFP; CaSR^{p190/+}* x *Tg(UAS:CaSR-EGFP); CaSR^{p190/+}* adults. In all cases, transgenic larvae were compared to their non-transgenic siblings to control for genetic background effects on behavior.

Dose-dependent rescue strength analysis

Tg(α-tubulin:gal4,myl7:GFP);[78] *Tg(UAS:CaSR-EGFP); CaSR^{p190/+}* fish were incrossed or crossed to *Tg(UAS:CaSR-EGFP); CaSR^{p190/+}* to produce larvae. Larvae were sorted for expression strength at 3 dpf. Larvae with barely-visible CNS expression or expression only in the PNS were discarded. The remaining larvae were sorted into "no neuronal expression," "low neuronal expression," and "high neuronal expression" groups subjectively by the experimenter. Larvae were assayed for behavior at 5 dpf and subsequently genotyped as described above.

Imaging y234 neurons

We crossed *Et(y234:Gal4)*; *Tg(UAS:CaSR-EGFP)* to *Tg(hspGFF62a:Gal4)*[57]; *Tg(UAS:gap43-citrine)*[56] adults and sorted for green larvae on a fluorescent dissecting microscope at 2 dpf. We bleached larvae, immunostained for tERK, and performed confocal imaging on a Zeiss 880 microscope as described above in the MAVEN protocol. Gap43-citrine retained its fluorescence throughout the staining protocol without the need for additional antibody staining. Images were acquired at 1.5 or 2X digital zoom, and z stack images were taken 0.84 um apart. To quantify the y234/DCR6 and y234/NP4 projections to the Mauthner, we tallied the number of larvae that had a given projection type and divided this by the total number of larvae in which both the y234 population and at least one Mauthner neuron were labeled. Pseudocoloring and background subtraction were performed using the 3D Image Viewer plugin in FIJI to create a separate stack for each desired channel, then merging the stacks with separate colors.

Multivariate Analysis of Variegated Expression in Neurons (MAVEN)

Our Multivariate Analysis of Variegated Expression in Neurons (MAVEN) strategy consisted of four steps: separation of larvae by their behavior, immunostaining, confocal imaging, and image analysis.

Behavior (for MAVEN)

Tg(α-tubulin:gal4,myl7:GFP); *Tg(UAS:CaSR-EGFP)*; *CaSR*$^{p190/+}$ fish were incrossed or crossed to *Tg(UAS:CaSR-EGFP); CaSR*$^{p190/+}$ to produce larvae. Larvae were sorted for green expression in the CNS on d3 and assayed for behavior on at 5 dpf. Behavioral analysis was used to identify larvae with SLC-shifted behavior in response to thirty 1500 Hz 25.5 dB stimuli, which typically elicits mostly LLCs (RBB < −50). Larvae with RBB of >50 were considered SLC-shifted, with <-50 RBB unshifted. To ensure reliability of the measured RBB, only larvae that responded to >40% of stimuli (n = 12 responses) were included.

Immunostaining (MAVEN)

After behavior was assayed, larvae were stored in methanol for <48 h. Behavioral phenotypes were calculated and larvae were marked as having the SLC-shifted or unshifted phenotype by specific cut patterns to their tails, then all larvae of both phenotypes and all genotypes from a single test date were fixed in a single tube overnight in 4% PFA in PBS at 4°C. After three 5-min PBT washes, they were then bleached in 3% hydrogen peroxide and 1% w/v potassium hydroxide at 55° for approximately 5–10 min, until melanophores were no longer visible and eyes were pale yellow-orange in color. Next they were incubated in 150mM Tris-HCl pH 9.0 for 15 min at 70°C, permeabilized in trypsin on ice for 45 min, washed, incubated in block (2% Normal Goat Serum, 1% BSA, 1% DMSO in PBT) for 1 h at room temperature, incubated in primary antibody (Rockland Chicken anti-GFP 600-901-B12 1:200; Cell Signaling mouse anti-tERK, #4696, 1:500) overnight at 4°C, and washed three times in PBT for 15 min each. Secondary antibody (Jackson ImmunoResearch donkey anti-chicken Alexa 488, 703-545-155, 1:200; Invitrogen goat anti-mouse IgG1 Alexa 633, A21126, 1:500) was also applied overnight at 4°C. After washing off secondary three times in PBT for 15 min each, larvae were stored in a 2:1 mixture of Vectashield and PBS until imaging. A detailed protocol is provided in Randlett et al. 2015.[52]

Confocal imaging (MAVEN)

Larvae were mounted in 1.25% low-melt agarose and imaged on a 20X air objective on a Zeiss 880 confocal microscope. Images were tiled to capture an area spanning from the rostral spinal cord to the olfactory epithelium. All settings were kept consistent within a given imaging date, although staining was sufficiently different between tubes that different settings were used across dates. In postprocessing, signal was normalized by the average signal of all larvae that were stained in a single tube to mitigate tube effects. Larvae were genotyped for *CaSR*^{p190} after imaging.

Image analysis (MAVEN)

Confocal stacks were registered to a 3D anatomical atlas as described[52] via their tERK stain to the reference tERK stain using FIJI's CMTK registration pipeline and GUI (https://github.com/sandorbx/Fiji-CMTK-registration-runner-GUI). Next, area-normalized GFP signal in each brain region for each larva imaged was extracted using a modified version of the MakeTheMAPMap function,[52] QuantifySignalMultipleBrains. GFP signal was not normalized to tERK signal.

Next, data were imported to R. Signal from all regions within or posterior to Rhombomere 7 were excluded due to inconsistent alignment to the reference brain in these regions. Analysis including these regions returned the same results as analysis without them. Next, LASSO regression[53] was performed on CaSR WT larvae to determine the brain regions in which signal best predicted whether brains fell into the "SLC-shifted" or "not SLC-shifted" category. The hyperparameter lambda was determined by fourfold cross-validation using the cv.glmnet function from the glmnet package. two-way ANOVA was performed on all successfully-genotyped larvae that responded to weak stimuli with a defined phenotype of either "not SLC-biased" or "SLC-biased" (n = 140 total larvae).

QUANTIFICATION AND STATISTICAL ANALYSIS

Statistical analysis was performed in a combination of Microsoft Excel, R, and PRISM 7, 8, and 9 (GraphPad). The D'Agostino & Pearson test was used to assess normality. If data were not normal and ns were <50, the Mann-Whitney test was used for comparisons between two groups or Kruskall-Wallis test with Dunn's multiple comparisons for comparisons between multiple groups. If data were normally distributed or ns were >50, the student's T test was used for comparisons between two groups or one-way ANOVA for comparisons between multiple groups.